 DOI: 10.3217/978-3-85125-663-5-33

Motion Artefact Compensation for Multi-Line Scan Imaging

Nicole Brosch[1], Svorad Štolc[1], Simon Breuss[1], Doris Antensteiner[1]

***Abstract*— This work focuses on the compensation of transport synchronization artefactes that may occur during multi-line scan acquisitions. We reduce these motion artefactes by a warping function that stretches/squeezes line frames in the scanning domain that were acquired too early/late. The estimation of the warping function is controlled by comparing light field views and enforce uniform spacing between line acquisitions. This approach enables multi-line scan systems to perform multi-line scan light field imaging largely independent from the transport and trigger quality.**

I. INTRODUCTION

Line scan imaging is a popular choice when performing industrial quality inspection [4]. However, when capturing moving objects *motion artefacts* may arise when the transport velocity of the object is not perfectly synchronized with the camera [4], [6], [8]. While in conventional line scanning (i.e., single line) such artefacts are not distinguishable from the correct signal, they become visible in light fields acquired with a multi-line scan system [6] (Figure 1). The standard solution to motion artefacts in line scan imaging, is to use high-end hardware components, such as high-precision transport stages and motion sensors [4]. However, we have observed that despite such hardware, acquisitions might sill suffer from such artefacts especially at high magnifications. The importance of compensating for motion artefacts was stressed by existing line scan imaging approaches (e.g., [4], [6], [8]) and addressed in a multi-line scenario in [1], i.e., the approach spotlighted in this paper. Related works outside the realm of line scanning, include motion compensation based on explicitly recorded reference patterns [5], [7].

II. ALGORITHM DESCRIPTION

A light field acquired with [6] is stored in an EPI stack $V \in \mathbb{R}^{n\times m\times r}$ (Figure 1). In $V(x_i, v_k, y_j)$ a moving object was captured at n space instances and with m camera lines that consist of r pixels, where $1 \le i \le n$, $1 \le k \le m$ and $1 \le j \le r$. If the transport velocity is not perfectly synchronized with the multi-line scan camera, the distance between successive acquired lines is not constant. This leads to distortions of the assumed integer indices x_i and true sub-pixel indices $\tilde{x}_i$. To compensate for motion artefacts, i.e., the discrepancy between x_i and $\tilde{x}_i$, we first determine $\tilde{x}_i$, and then unwarp pixels in V to generate a new EPI stack, with uniform distances between its position indices $\tilde{x}_i$. To find the true sub-pixel indices $\tilde{x}_i$, that correspond to each observed index x_i, we formulate an energy function,

$$\min_{\tilde{x}} \frac{1}{2}\|E_d(\tilde{x})\|^2 + \frac{\lambda_1}{2}\|E_x(\tilde{x})\|^2 + \frac{\lambda_2}{2}\|E_s(\tilde{x})\|^2. \quad (1)$$

[1]AIT Austrian Institute of Technology, Giefingasse 4, 1210 Vienna, Austria firstname.lastname@ait.ac.at

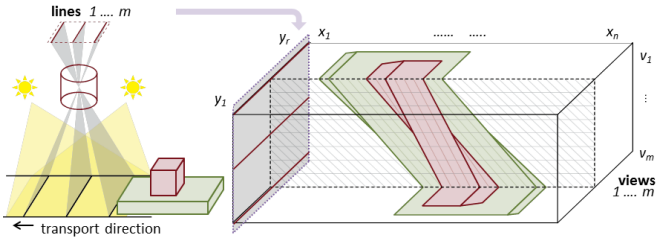

Fig. 1. Illustration of multi-line scan image acquisition setup [6] (left). At each space instance a set of m lines is captured, then the object is moved by a linear transport stage. Multi-line frames with position index x_i are acquired simultaneously. Each camera line captures the object under a different viewing angle and, over the time, contributes to a different view of the object. Each view v_k, consists of line acquisitions with indices x_i. The views compose a linear light field, which is stored in an *epipolar plane image* (EPI) stack $V_{y_j}(x_i, v_k)$ [3] (right). Figure taken from [6].

consisting of a *disparity term* E_d, an *identity term* E_x and a *smoothness term* E_s, which will be discussed in more detail below. Here, λ_1 and λ_2 are used to balance the energy terms.

The *disparity term* is based on the observation that motion artefacts become visible in 3D reconstructions (e.g., Figure 2, a) from light fields acquired with [6]. An object point and an entire multi-line frame associated with x_i that was performed too early/late, causes a smaller/larger disparity than expected. In order to determine a true index $\tilde{x}_i$, we use estimated disparities to locate corresponding multi-line frames in different views and adjust the position of the i-th mutli-line frame from x_i to $\tilde{x}_i$. More precisely, this adjustment is based on balanced forward and backward disparities between two views, i.e., forward disparities between views v_k and v_{k+1} and backward disparities between views v_k and v_{k-1} (Figure 3). In order to speed up the approach, we determine the mean forward disparity $d_{k,i}$ and the mean backward disparity $\bar{d}_{k,i}$ in each index x_i. Given $d_{k,i}$ and $\bar{d}_{k,i}$ for each position index x_i, we infer the true indices $\tilde{x}_i$ with:

$$E_d(\tilde{x}) = D'\tilde{x}, \quad (2)$$

where for each position index x_i for which both forward and backward disparities exist, we form one line in matrix $D' \in \mathbb{R}^{n\times n}$. The corresponding set of linear equations in Eq. (1) for any given view v_k $k \in \{2,\ldots,m-1\}$ are:

$$\begin{aligned} -2\tilde{x}_i + \tilde{x}_{i+\lfloor d_{k,i}\rfloor}(1 - d_{k,i} + \lfloor d_{k,i}\rfloor) + \tilde{x}_{i+\lceil d_{k,i}\rceil}(d_{k,i} - \lfloor d_{k,i}\rfloor) \\ + \tilde{x}_{i+\lfloor \bar{d}_{k,i}\rfloor}(1 - \bar{d}_{k,i} + \lfloor \bar{d}_{k,i}\rfloor) + \tilde{x}_{i+\lceil \bar{d}_{k,i}\rceil}(\bar{d}_{k,i} - \lfloor \bar{d}_{k,i}\rfloor) \\ \approx 0, \forall i \in \{1,\ldots,n\}. \quad (3) \end{aligned}$$

E_d may be generalized e.g., by including calibration information or when exchanging the L2 with an L1 penalization.

The *identity term* assumes that the actual movement is similar to the assumed ideal movement of the transport stage

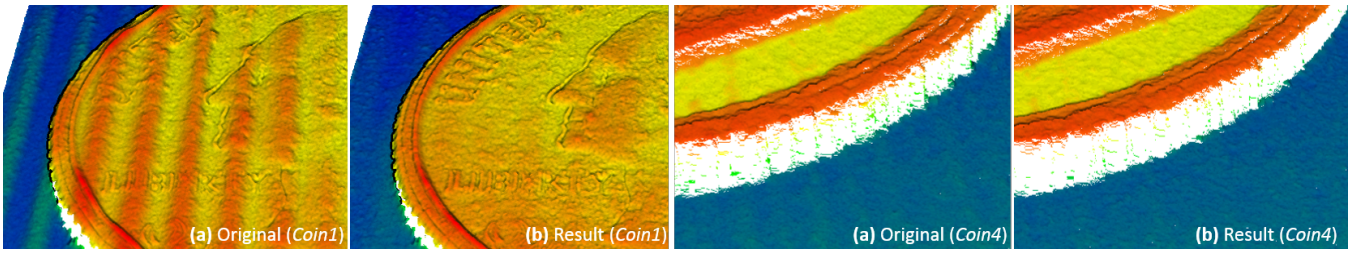

Fig. 2. Visual comparison of 3D reconstructions generated from original (a) and undistorted (b) light field acquisition of coins. Ripples due to motion artefacts in (a) are significantly reduced in (b). For the left example, a camera in free-running mode was used to increase the visibility of motion artefacts.

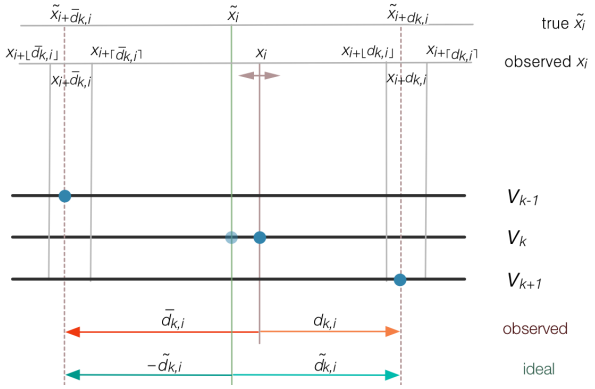

Fig. 3. Illustration of E_d. Disparities relate corresponding object points (dark blue) in different views (v_{k-1}, v_k, v_{k+1}). In presence of transport issues, points are acquired too early/late (light vs. dark blue point in v_k) and the observed index x_i differs from its true index $\tilde{x}_i$. In an ideal EPI stack (perfect transport synchronization) fore- and backward disparities are balanced ($\tilde{d}_{k,i}$, green arrows). In a distorted EPI stack with observed x_i and disparities $\bar{d}_{k,i}$ and $d_{k,i}$ (red and orange arrow) this is not the case. For x_i, $\tilde{x}_i$ can be determined by enforcing the balance between $\tilde{x}_{i+\bar{d}_{k,i}}$ and $\tilde{x}_{i+d_{k,i}}$.

up to a non-accumulative normally distributed error:

$$E_x(\tilde{x}) = x - \tilde{x}. \tag{4}$$

Hence in Eq. (1), we also solve the set of equation:

$$x_i - \tilde{x}_i \approx 0, \quad \forall i \in \{1,...,n\}. \tag{5}$$

The *smoothness term* ensures a smooth solution by penalizing abrupt changes between neighboring $\tilde{x}_i$:

$$E_s(\tilde{x}) = \Delta\tilde{x}, \tag{6}$$

where Δ denotes the Laplacian operator, which is implemented in form of a convolution filter with the kernel $[1,-2,1]$. Thus, we form another set of linear equations:

$$-2\tilde{x}_i + \tilde{x}_{i-1} + \tilde{x}_{i+1} \approx 0, \quad \forall i \in \{1,...,n\}. \tag{7}$$

We express the energy term in Eq. (1) as an overdetermined linear system of equations, which can be solved approximately using a standard least squares solver.

III. EXPERIMENTAL RESULTS

We perform evaluations on EPI stacks acquired with [6]. To increase the visibility of motion artefacts, our experiments are also performed on a *free running dataset*, for which camera and transport are not synchronized via trigger. In Table I, we compare disparity maps that were generated from the original and from our undistorted EPI stacks. Since disparity values in such a (assumed flat) region should be constant, the standard deviation can be used as a quality measure, where low values indicate less artefacts than larger ones. Table I also contains an analogue evaluation for depth maps obtained with the calibrated system [2] and our compensation approach which includes the calibration information. In our dataset, the proposed compensation approach significantly reduces the motion artefacts (Figure 2, Table I).

TABLE I

EVALUATION: STANDARD DEVIATIONS OF DISPARITIES/DEPTHS IN FLAT REGION BEFORE (ORIGINAL) AND AFTER (RESULT) COMPENSATION

free-running camera			**synchronization via trigger**		
Data set	Original	Result	Data set	Original	Result
Note1	0.3061	0.0986	*Coin3*	0.0686	0.0617
Note2	0.2896	0.1153	*NoObject1*	0.0612	0.0481
PCB1	0.3069	0.1283	**calibrated system** (depth)		
PCB2	0.3361	0.1319	Data set	Original	Result
Coin1	0.2954	0.0992	*Coin4*	0.0147	0.0137
Coin2	0.2771	0.0912	*NoObject2*	0.0161	0.0133

IV. CONCLUSION

The compensation of motion artefacts allows multi-line scan light field imaging when the transport cannot be controlled with high precision. The compensation approach constrained the transport position indices according the information obtained by comparing multiple views and enforced uniform spacing between line acquisitions. The undistorted views were computed according to a warping function, which significantly reduced artefacts in our test data.

REFERENCES

[1] N. Brosch et al., "Warping-based motion artefact compensation for multi-line scan light field imaging", *EI'18*, 2018, pp.273-1-273-6.
[2] B. Blaschitz et al., "Geometric calibration and image rectification of a multi-line scan camera for accurate 3D reconstruction", *EI'18*, 2018, pp.240-1-240-6.
[3] R. Bolles et al., "Epipolar-Plane Image Analysis: An approach to determining structure from motion", *IJCV'87*, 1, 1, 1987.
[4] R. Davies, *Machine Vision: Theory, Algorithms, Practicalities.* Morgan Kaufmann Publishers Inc., 2004.
[5] B. Krolla et al., "Light field from smartphone-based dual video", *ECCV'14*, 2014, pp. 600-610.
[6] S. Štolc et al., "Depth and all-in-focus imaging by a multi-line-scan light-field camera," *Journal of Electronic Imaging*, 23, 5, 2014.
[7] T. Weise et al., "Fast 3D scanning with automatic motion compensation", *CVPR'07*, 2007, pp. 1-8.
[8] H. Yuet al., "An antivibration time-delay integration CMOS image sensor with online deblurring algorithm", *TCSVT*, 26, 8, 2016.